



Highly Regioselective Amination of Unactivated Alkanes by Hypervalent Sulfonylimino- λ^3 -Bromane

Masahito Ochiai *et al.*

Science **332**, 448 (2011);

DOI: 10.1126/science.1201686

This copy is for your personal, non-commercial use only.

If you wish to distribute this article to others, you can order high-quality copies for your colleagues, clients, or customers by [clicking here](#).

Permission to republish or repurpose articles or portions of articles can be obtained by following the guidelines [here](#).

The following resources related to this article are available online at www.sciencemag.org (this information is current as of September 13, 2012):

Updated information and services, including high-resolution figures, can be found in the online version of this article at:

<http://www.sciencemag.org/content/332/6028/448.full.html>

Supporting Online Material can be found at:

<http://www.sciencemag.org/content/suppl/2011/04/20/332.6028.448.DC1.html>

This article **cites 26 articles**, 1 of which can be accessed free:

<http://www.sciencemag.org/content/332/6028/448.full.html#ref-list-1>

This article appears in the following **subject collections**:

Chemistry

<http://www.sciencemag.org/cgi/collection/chemistry>

Highly Regioselective Amination of Unactivated Alkanes by Hypervalent Sulfonylimino- λ^3 -Bromane

Masahito Ochiai,^{1*} Kazunori Miyamoto,¹ Takao Kaneaki,¹ Satoko Hayashi,² Waro Nakanishi^{2*}

Amination of alkanes has generally required metal catalysts and/or high temperatures. Here we report that simple exposure of a broad range of alkanes to *N*-triflylimino- λ^3 -bromane **1** at ambient temperature results in C–H insertion of the nitrogen functionality to afford triflyl-substituted amines in moderate to high yields. Marked selectivity for tertiary over secondary C–H bonds was observed; primary (methyl) C–H bonds were inert. Addition of hexafluoroisopropanol to inhibit decomposition of **1** dramatically improved the C–H amination efficiencies. Second-order kinetics, activation parameters (negative activation entropy), deuterium isotope effects, and theoretical calculations suggest a concerted asynchronous bimolecular transition state for the metal-free C–H amination event.

Direct and selective functionalization of alkane C–H bonds constitutes a long-standing goal in synthetic organic chemistry (1–5). Alkanes are major constituents of petroleum and natural gas, but they are relatively inert and tend to be functionalized on a commercial scale through an inefficient sequence of overoxidation followed by reduction. Over the past several decades, however, substantial progress has been reported, primarily through the use of transition metal-catalyzed processes.

We focus here on the selective transformation of ubiquitous but unactivated aliphatic (sp³) C–H bonds to amines and amides. Both free-nitrene insertions and metal-nitrenoid aminations have been reported (Fig. 1A); in general, however, free-nitrene processes are unselective and uncontrollable and, as a result, are of little synthetic value. Therefore, the discovery by Breslow and Gellman of the capacity of Mn and Fe tetraphenylporphyrin complexes to catalyze the tosylation of cyclohexane (**2b**) using *N*-tosylimino- λ^3 -iodane was a promising development (6). Recently, Fiori *et al.* and some other groups greatly extended this methodology and have found an efficient method for Rh-catalyzed high-yield amination of **2b** using in situ-generated imino- λ^3 -iodane, indicating the powerful nature of the transition metal-catalyzed amination of aliphatic C–H bonds (7–10).

Hypervalent aryl- λ^3 -bromanes exhibit higher reactivity compared with aryl- λ^3 -iodanes (the λ^3 notation indicates that the bromine and iodine centers exceed their standard valence by two) (11). This is probably due to the greater electronegativity as well as the larger ionization potential of bromine relative to iodine (12–14). Recently, we reported synthesis of hypervalent *N*-(trifluoromethyl-

sulfonyl)imino- λ^3 -bromane **1** (15); the iminobromane **1** serves as an active organo nitrenoid species and directly undergoes stereospecific aziridination of olefins with retention of stereochemistry and transylation to iodobenzenes, pyridines, and sulfides (16). In marked contrast to the reactions of imino- λ^3 -iodanes, all of these reactions do not require the use of any transition-metal catalysts and proceed smoothly, even at room temperature. These results suggest that **1** might be a more active aminating agent of aliphatic C–H bonds, perhaps even obviating the need for a catalyst.

N-(trifluoromethylsulfonyl)imino- λ^3 -bromane **1** was prepared by stoichiometric ligand exchange of the fluorines in aryl(difluoro)- λ^3 -bromane *p*-CF₃C₆H₄BrF₂ with triflylamide (TfNH₂) in acetonitrile at 0°C in a polytetrafluoroethylene perfluoroalkoxy (Teflon PFA, DuPont, Wilmington, DE) vessel (15, 17, 18). Compound **1** is sparingly soluble in cyclohexane (**2b**) but smoothly transfers the nitrene unit (NTf) to the alkane. Stirring a 0.01 M suspension in cyclohexane at ambient temperature gradually dissolves the bromane **1**, leading to selective insertion of the nitrogen functionality into the unactivated methylene C–H group. After stirring for 24 hours, *N*-(cyclohexyl) triflylamide (**3b**) was isolated in 91% yield (Fig. 1B). This reactivity is in marked contrast with the reported amination of cyclohexane using imino- λ^3 -

iodanes PhI=NSO₂Ar (7–10), which requires activation by a transition-metal catalyst (Rh, Cu, or Ag), and with amination by *p*-toluenesulfonyl azide, which requires heating to 165°C to generate the reactive nitrene (19).

Five-, seven-, and eight-membered cyclic alkanes similarly afforded high yields of *N*-triflylamides **3** at room temperature under metal-free conditions. Somewhat decreased yields were obtained in the reaction of cyclodecane (**2e**) and cyclopentadecane (**2f**) (Fig. 1B).

We next explored the scope of aminations using **1** with acyclic and substituted cyclic alkanes (Table 1). Acyclic alkanes **2 g–i** afforded moderate to good yields (34 to 74%) of amines **3**, whereas 2,2,4,4-tetramethylpentane (**2m**) was recovered unchanged, though decomposition of imino- λ^3 -bromane **1** was observed in this case, with formation of TNH₂ (91%) and *p*-CF₃C₆H₄Br (89%) (Table 1, entry 13). The use of excess amounts (20 equivalents relative to **1**) of hexafluoroisopropanol (HFIP) as an additive dramatically improved the C–H amination efficiencies, affording good to excellent yields of amides **3** (compare Table 1 entries 3/4, 5/6, 7/8, and 9/10) while maintaining similar site selectivities; even 2,3-dimethylbutane (**2l**) with a sterically encumbered 3° C–H site afforded a high yield of amination product in the presence of HFIP (entry 12). Computational and kinetic studies suggest that HFIP slows down the rate of decomposition of imino- λ^3 -bromane **1** via formation of a 1:1 complex through hydrogen-bonding interactions (see figs. S1 to S3 and SOM text) (20).

In *n*-hexane (**2g**), amination of the secondary C2-H and C3-H bonds occurred with comparable selectivities. In branched alkanes, however, a notable preference for tertiary over secondary C–H bonds was observed in most cases, except in the reactions of norbornane (**2o**) and *trans*-decalin (**2t**). No primary (methyl) C–H reactivity was observed in any of the substrates examined. Differences in C–H bond dissociation energies account reasonably well for these site selectivities (fig. S4 and SOM text). Norbornane (**2o**) exclusively undergoes C–H insertion at the 2° C2-H site (with high exo selectivity), though in this case the 3° C1-H bond is strengthened by the rigid structure around C1. A similar preference for oxyfunctionalization

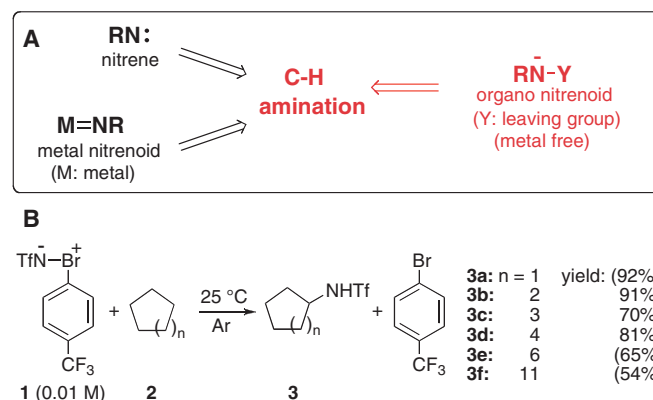


Fig. 1. (A) Strategy for unactivated C–H amination. R, arenesulfonyl, alkane-sulfonyl, alkoxysulfonyl, etc. (B) C–H amination of cycloalkanes with *N*-triflylimino- λ^3 -bromane **1** under metal-free conditions at room temperature. Yields shown in parentheses were determined by GC; otherwise, isolated yields are reported. Tf = CF₃SO₂.

¹Graduate School of Pharmaceutical Sciences, University of Tokushima, 1-78 Shomachi, Tokushima 770-8505, Japan. ²Department of Material Science and Chemistry, Faculty of Systems Engineering, Wakayama University, 930 Sakaedani, Wakayama 640-8510, Japan.

*To whom correspondence should be addressed. E-mail: mochiai@ph.tokushima-u.ac.jp

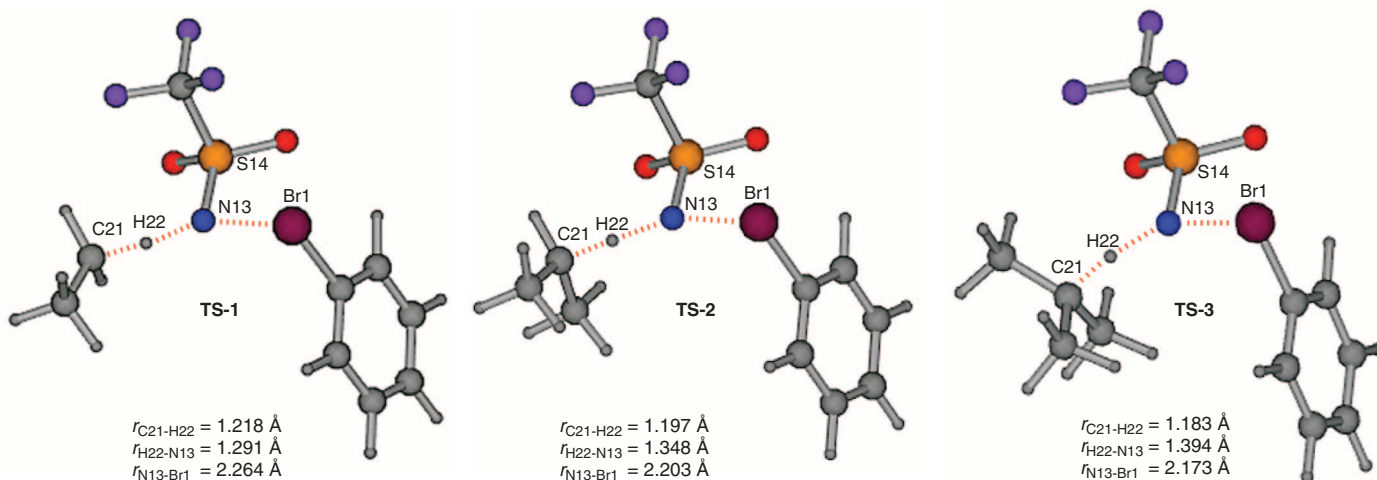
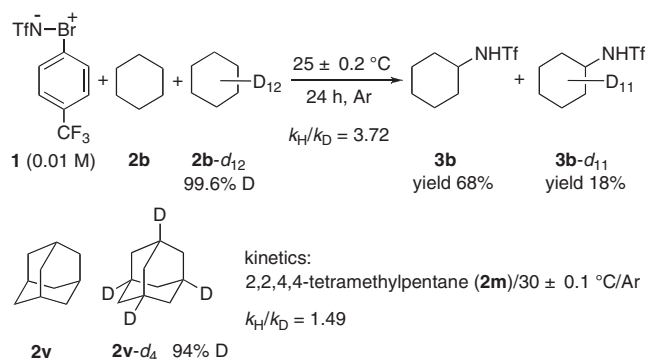


Fig. 2. Transition state structures for C–H aminations of ethane (**TS-1**), propane (**TS-2**), and isobutane (**TS-3**) with PhBr=Ntf **4** optimized at the MP2/6-311+G(d) (Br, S, N) and 6-31G(d,p) (F, O, C, H) levels. r , bond length.

Fig. 3. Deuterium kinetic isotope effects for C–H aminations. D, deuterium.



at C2 and for exo stereoselectivity was observed in norbornane oxidation with dioxiranes (**21**) and oxaziridines (**22**). Silver-catalyzed amination of simple alkanes with imino- λ^3 -iodane showed a close parallel $3^\circ > 2^\circ > 1^\circ$ selectivity (**23**).

Steric hindrance due to the bulky aryl- λ^3 -bromanyl and triflyl groups attached to the nitrogen atom of **1** also seems to influence the relative substrate reactivities and positional selectivities. For instance, the sterically congested methylene group of tetramethylated pentane **2m** undergoes no amination (facilitating the use of **2m** as an inert solvent for amination of solid substrates such as **2o** and **2v**). Differences in $3^\circ/2^\circ$ site selectivities for *trans*- (**2r**) and *cis*-1,2-dimethylcyclohexane (**2s**) as well as *trans*- (**2t**) and *cis*-decalin (**2u**) (with both *cis*-isomers showing higher 3° selectivity) probably reflect differences in steric hindrance and/or strain release on approaching the transition state of the amination (Table 1, entries 18 to 21) (**24**). These considerations were supported by competition experiments that exposed **1** simultaneously to *trans*- (**2p**) and *cis*-1,4-dimethylcyclohexane (**2q**): The equatorial tertiary C–H bond reacts 4.4 times more rapidly than those oriented axially (fig. S5). Hence, a subtle balance of electronic and steric factors seems to determine

the relative rates of C–H insertion and associated regioselectivity.

The stereochemistry of *trans*-**3pa** and *cis*-**3qa** was determined by conversion of the TfN-substituted dimethylcyclohexanes to the known mesylamides through *N*-benzylation, β elimination of TfH, NaBH₄ reduction, debenylation, and finally mesylation (figs. S6 and S7). These results clearly indicated exclusive retention of the starting stereochemistry of **2p** and **2q** in the products.

Rates for C–H amination of alkanes with imino- λ^3 -bromane **1** (9.5×10^{-5} M, where a clear solution of **1** was obtained) at 30°C were measured spectrophotometrically under pseudo-first-order conditions using inert tetramethylpentane **2m** as a solvent (tables S1 and S2). In all cases examined, the observed rate constants k_{obs} proved proportional to the concentration of alkane and the slopes of such plots afforded the second-order rate constants ($k_2/\text{M}^{-1}\text{s}^{-1}$): 0.000778 (**2a**), 0.000989 (**2b**), 0.00127 (**2o**), and 0.0289 (**2v**). The observed second-order rate law suggests the likely involvement of a bimolecular transition state. For each compound, second-order rate constants k_2 (CH₂) for methylene groups and k_2 (CH) for methine groups were calculated based on the product profiles shown in Table 1; relative reactivities of each hydrogen atom, obtained after statistical

correction for differing numbers of H atoms in each substrate, are shown in Table 1.

Adamantane (**2v**) is the most reactive substrate that we examined. The magnitude of reactivities of 3° C–H bonds relative to cyclohexane (**2b**) varies widely, from an 81-fold enhancement for adamantane (**2v**) to a 3.5-fold increase for dimethylpentane (**2j**). These results again demonstrate that, in molecules where C–H bonds of similar electron densities are present, sterics can play a major role in guiding selectivity.

The second-order kinetics for reaction of **1** with alkanes suggest that generation of free nitrene is not rate limiting (and may not even be on the pathway). Theoretical calculations on the reactions of phenyl(imino)- λ^3 -bromane PhBr=Ntf **4** with ethane, propane, and isobutane also predict that the generation of singlet nitrene is higher in energy than bimolecular C–H amination pathways, in which iminobromane **4** functions as an active nitrenoid species (fig. S11). The calculated activation barriers (in kilocalories per mole) for C–H insertion with **4** showed a monotonic but large decrease in the order Et–H (22.5), *i*-Pr–H (17.1), and *t*-Bu–H (13.1), which parallels the experimentally obtained relative reactivities of C–H bonds. The TfN insertion (**TS-2**) into the secondary center in propane by **4** proceeds with a barrier of only 17.1 kcal mol^{−1}, which is very close to the evaluated activation enthalpy (ΔH^\ddagger) of 19.4 kcal mol^{−1} for the reaction of cyclohexane (**2b**) with imino- λ^3 -bromane **1** (fig. S8). A moderate and negative activation entropy ($\Delta S^\ddagger = -8.38$ cal mol^{−1}K^{−1}) for the amination of cyclohexane (**2b**) indicates some loss of mobility in the transition state, in good agreement with a concerted bond-formation/scission process obtained by calculations.

In each of the calculated C–H amination transition states **TS-1** (ethane insertion), **TS-2** (propane CH₂ insertion), and **TS-3** (isobutane CH insertion), the alkane moiety (RH, where R is Et, *i*-Pr, *t*-Bu) becomes positively charged (by +0.2806, +0.2235, and +0.1914, respectively),

whereas the total positive charge (+0.8816) of the PhBr moiety in **4** decreases to +0.3754, +0.4524, and +0.4896, respectively (Fig. 2). These results suggest transfer of alkane C–H σ -bonding electrons to iminobromane **4** with some hydride-transfer character. Although the C21–H22 bond

activation and the N13–C21 bond formation take place as a single event, **TS-1** to **TS-3** indicate a highly asynchronous transition state, with N13–H22 bond formation being much more advanced than N13–C21 bond formation (Fig. 2). These transition-state structures are reminiscent of those calculated for the concerted alkane C–H insertions by dimethyldioxirane (**25**) and rhodium-carbene/nitrene complex (**26**, **27**). As observed for *trans*-(**2p**) and *cis*-1,4-dimethylcyclohexane (**2q**), the aminations proceed with full retention of stereochemistry, indicating that long-lived carbocation or free radical intermediates are not involved in the aminations.

Deuterium kinetic isotope effects (KIEs) were evaluated by the competitive reaction of imino- λ^3 -bromane **1** with a 1:1 mixture of cyclohexane (**2b**) and cyclohexane- d_{12} (**2b-d₁₂**) at 25°C: A primary deuterium KIE k_H/k_D (k_H , rate constant of **2b**; k_D , rate constant of **2b-d₁₂**) of 3.72 for 2° C–H insertion was determined by gas chromatography (GC) (Fig. 3). Comparison of k_2 values (table S1) for 3° C–H insertion of adamantane (**2v**) and 1,3,5,7-tetradeuterioadamantane (**2v-d₄**) in tetramethylpentane **2m** at 30°C afforded a smaller k_H/k_D value of 1.49 (**28**). These moderate KIE values suggest only partial C–H bond breaking in the transition state and are not compatible with a hydrogen atom abstraction/radical-rebound mechanism, as proposed for Ru- and Cu-nitrenoid-based C–H aminations with large KIEs of 6.1 to 6.6 (**29**, **30**). The smaller KIE value observed for the tertiary C–H bonds of **2v** relative to the secondary C–H bonds of **2b** is consistent with the calculations, which show greater extension of the breaking C21–H22 and N13–Br1 bonds in **TS-2** than in **TS-3** (Fig. 2); the latter structure reflects the more early character of the transition state. We feel that these KIEs—together with the second-order kinetics, kinetic parameters (negative activation entropy), retention of stereochemistry, and theoretical calculations—strongly implicate a concerted asynchronous pathway for metal-free C–H amination with sulfonylimino- λ^3 -bromane **1**. The driving force for this room-temperature uncatalyzed insertion into unactivated alkane C–H bonds is probably the greatly enhanced nucleofugality of aryl- λ^3 -bromanyl groups compared with aryl- λ^3 -iodanyl groups, which correlates with increased instability of hypervalency at bromine relative to iodine (**31–33**).

Table 1. Metal-free C–H amination at room temperature with imino- λ^3 -bromane **1**. Unless otherwise noted, 0.01 M of **1** (with 20 equivalents of HFIP, where indicated) was stirred in neat alkane under Ar for 10 to 24 hours. Yields and ratios of the indicated products **3** (major isomer on the left) were determined by GC (numbers in parentheses are isolated yields of the major product; *N* = NHTf). Relative reactivities of C–H bonds compared with cyclohexane (**2b**) after statistical correction (per H atom) are shown in red (methine groups) and blue (methylene groups).

Entry	Alkane 2	Additive (equiv)	Product 3	Yield (%)	Ratio
1		2g , -		51	57:43
2		2g , HFIP		55 (55)*	57:43
3		2h , -		42	95:5
4		2h , HFIP		72 (47)	94:6
5		2i , -		46	97:3
6		2i , HFIP		91 (79)	97:3
7		2j , -		34	97:3
8		2j , HFIP		64 (51)	97:3
9		2k , -		74	86:14
10		2k , HFIP		96 (78)*	86:14
11		2l , -		44	
12		2l , HFIP		78 (55)	
13		2m , -		0	
14		2n , -		84 (76)*	82:18
15†		2o , HFIP		67 (61)*	89:11
16		2p , -		64 (62)*	81:19
17		2q , -		66 (60)*	86:14
18		2r , -		71 (66)*	52:48
19		2s , -		92 (77)	96:4
20		2t , -		45 (8)	29:71
21		2u , -		78 (58)	86:14
22†		2v , -		(86)*	92:8
23†		2w , R = Me, R' = H		(62)*	92:8
24†		2x , R = Et, R' = H		(80)*	91:9
25†		2y , R = R' = Me		(69)	93:7

*Total isolated yields of products **3**. † Bromane **1** (0.02 M) and alkane (100 to 400 equiv) were mixed in tetramethylpentane **2m** solvent.

References and Notes

- J. A. Labinger, J. E. Bercaw, *Nature* **417**, 507 (2002).
- K. Godula, D. Sames, *Science* **312**, 67 (2006).
- A. A. Fokin *et al.*, *J. Am. Chem. Soc.* **122**, 7317 (2000).
- H. M. L. Davies, J. R. Manning, *Nature* **451**, 417 (2008).
- P. R. Schreiner, A. A. Fokin, *Chem. Rec.* **3**, 247 (2004).
- R. Breslow, S. H. Gellman, *J. Chem. Soc. Chem. Commun.* **1982**, 1400 (1982).
- M. R. Fructos, S. Trofimenko, M. M. Díaz-Requejo, P. J. Pérez, *J. Am. Chem. Soc.* **128**, 11784 (2006).
- Z. Li, D. A. Capretto, R. Rahaman, C. He, *Angew. Chem. Int. Ed.* **46**, 5184 (2007).
- K. W. Fiori, J. Du Bois, *J. Am. Chem. Soc.* **129**, 562 (2007).
- C. Liang *et al.*, *J. Am. Chem. Soc.* **130**, 343 (2008).
- U. Farooq, A.-H. A. Shah, T. Wirth, *Angew. Chem. Int. Ed.* **48**, 1018 (2009).

12. M. Ochiai, *Synlett* **2009**, 159 (2009).
13. Ionization potentials of halobenzenes increase in the order PhI (8.69 eV) < PhBr (8.98 eV) < PhCl (9.06 eV) (14).
14. D. R. Lide, Ed., *CRC Handbook of Chemistry and Physics* (CRC Press, Boca Raton, FL, 1992).
15. M. Ochiai *et al.*, *J. Am. Chem. Soc.* **129**, 12938 (2007).
16. M. Ochiai, K. Miyamoto, S. Hayashi, W. Nakanishi, *Chem. Commun.* **46**, 511 (2010).
17. Teflon PFA is a perfluoroalkoxy copolymer resin, available from DuPont, Wilmington, Delaware.
18. Materials and methods are available as supporting material on Science Online.
19. D. S. Breslow, M. F. Sloan, N. R. Newburg, W. B. Renfrow, *J. Am. Chem. Soc.* **91**, 2273 (1969).
20. C. Reichardt, *Solvents and Solvent Effects in Organic Chemistry* (Wiley-VCH, Weinheim, Germany, 2003).
21. R. Mello, M. Fiorentino, C. Fusco, R. Curci, *J. Am. Chem. Soc.* **111**, 6749 (1989).
22. D. D. DesMarteau, A. Donadelli, V. Montanari, V. A. Petrov, G. Resnati, *J. Am. Chem. Soc.* **115**, 4897 (1993).
23. B. P. Gómez-Emeterio, J. Urbano, M. M. Díaz-Requejo, P. J. Perez, *Organometallics* **27**, 4126 (2008).
24. K. Chen, A. Eschenmoser, P. S. Baran, *Angew. Chem. Int. Ed.* **48**, 9705 (2009).
25. M. N. Glukhovtsev, C. Canepa, R. D. Bach, *J. Am. Chem. Soc.* **120**, 10528 (1998).
26. E. Nakamura, N. Yoshikai, M. Yamanaka, *J. Am. Chem. Soc.* **124**, 7181 (2002).
27. X. Lin, C. Zhao, C.-M. Che, Z. Ke, D. L. Phillips, *Chem. Asian J.* **2**, 1101 (2007).
28. Small deuterium KIEs of 1.05 and 1.07 for the hydride abstraction reaction of the bridgehead adamantane C–H bond with tert-butyl cation and hydroperoxonium ion were reported (3).
29. S.-M. Au, J.-S. Huang, W.-Y. Yu, W.-H. Fung, C.-M. Che, *J. Am. Chem. Soc.* **121**, 9120 (1999).
30. Y. M. Badiei *et al.*, *Angew. Chem. Int. Ed.* **47**, 9961 (2008).
31. M. Ochiai, N. Tada, T. Okada, A. Sota, K. Miyamoto, *J. Am. Chem. Soc.* **130**, 2118 (2008).
32. T. Okuyama, T. Takino, T. Sueda, M. Ochiai, *J. Am. Chem. Soc.* **117**, 3360 (1995).
33. P. J. Stang, Z. Rappoport, M. Hanack, L. R. Subramanian, *Vinyl Cations* (Academic Press, New York, 1979).

Acknowledgments: This work was supported by a Grant-in-Aid for Scientific Research (B) (Japan Society for the Promotion of Science). We thank Central Glass Co., Japan, for a generous gift of BrF₃.

Supporting Online Material

www.sciencemag.org/cgi/content/full/332/6028/448/DC1

Materials and Methods

SOM Text

Figs. S1 to S12

Tables S1 and S2

References

14 December 2010; accepted 4 March 2011

10.1126/science.1201686

Global Trends in Wind Speed and Wave Height

I. R. Young,* S. Zieger, A. V. Babanin

Studies of climate change typically consider measurements or predictions of temperature over extended periods of time. Climate, however, is much more than temperature. Over the oceans, changes in wind speed and the surface gravity waves generated by such winds play an important role. We used a 23-year database of calibrated and validated satellite altimeter measurements to investigate global changes in oceanic wind speed and wave height over this period. We find a general global trend of increasing values of wind speed and, to a lesser degree, wave height, over this period. The rate of increase is greater for extreme events as compared to the mean condition.

Oceanic wind speed and wave height help to control the flux of energy from the atmosphere to the ocean (1) and upper ocean mixing (2). Thus, they substantially influence the mechanisms of air-sea interaction (3). Previous attempts to investigate trends in oceanic wind speed and wave height have used ship observations (4–8), point measurements (9), numerical modeling (10–15), or satellite observations (16). Almost all of these studies are regional rather than global. Although there is a range of results, many studies show an increasing trend in significant wave height, particularly in the North Atlantic and North Pacific, often correlated with interannual variations such as the North Atlantic Oscillation. Careful ship observations (4–6) also show waves locally generated by the wind (hereafter referred to as wind-sea) and swell behaving quite differently and that there exist quite different trends in wind speed and wave height. The present analysis uses recently developed satellite altimeter data sets to carefully investigate such trends on a global scale.

Satellite-based systems provide an alternative to visual or in situ measurements of oceanic wind

speed and wave height, using a variety of instruments, including altimeters, scatterometers, and synthetic aperture radar, providing global coverage of wind and/or waves. Of these instruments, the radar altimeter provides by far the longest-duration record. Since the launch of GEOSAT in 1985, there exists an almost continuous (there was a break in 1990–1991) record of measures from a total of seven different altimeter missions. Numerous calibrations of these altimeters have shown that the instruments can be used to measure significant wave height, $H_s = 4\sqrt{E}$, where E is the total energy of the wave field, with a root mean square (rms) error of less than 0.2 m (17), and wind speed, U_{10} , with a rms error of less than 1.5 m/s (17–21). Data from altimeter missions have been used to investigate mean ocean wind and wave climatology (21, 22) on a global scale. Recently, Zieger *et al.* (20) carried out systematic calibrations and cross-platform validations of all altimeter measurements over the full 23 years for which data are available. This study provided a consistent data set over this extended period. Because the data set spans multiple satellite platforms, consistent calibration and validation are critical when investigating long-term trends. In the present study, we used this data set to investigate whether there have been systematic changes in the ocean wind and wave climate over this

period. Because the seasonal cycle typically is large, care must be exercised in determining trend information from the data set [supporting online material (SOM)].

We aim here to determine whether there is a statistically significant trend [where trend is defined as a linear increase or decrease in the mean (23, 24)] within the time series of monthly mean, 90th-, and 99th-percentile values of wind speed and wave height for $2^\circ \times 2^\circ$ regions covering the globe. In the analysis, we take particular care to ensure that the trend can be separated from the seasonal component (SOM).

The trend was quantified as a linear function over the duration of the time series. The analysis revealed that 90th- and 99th-percentile wind speed data from the GEOSAT altimeter were of questionable quality (SOM). Therefore, these data were excluded from the analysis. As a result, the wave height analysis considers the period 1985–2008, whereas wind speed is analyzed for the shorter period 1991–2008. The trend was expressed for each $2^\circ \times 2^\circ$ region as the annual percentage increase or decrease relative to the mean condition and in absolute terms. The monthly mean, 90th-, and 99th-percentile trend values for both wind speed and wave height are shown in Figs. 1 to 3 (percentage increase or decrease) and Figs. S7 to S9 (SOM) (absolute increase or decrease), respectively.

There is a clear global increase in wind speed for all three statistics. The mean and 90th-percentile wind speed trends are relatively similar, with the magnitude of the increase being larger for the 99th percentile. Such a result indicates that the intensity of extreme events is increasing at a faster rate than that of the mean conditions. At the mean and 90th percentile, wind speeds over the majority of the world's oceans have increased by at least 0.25 to 0.5% per year (a 5 to 10% net increase over the past 20 years). The trend is stronger in the Southern Hemisphere than in the Northern Hemisphere. The only significant exception to this positive trend is the central north Pacific, where there are smaller localized increases in wind speed of approximately 0.25%

Swinburne University of Technology, Melbourne, Victoria, Australia.

*To whom correspondence should be addressed. E-mail: ir.young@anu.edu.au